AKADEMIA GÓRNICZO-HUTNICZA
IM. STANISŁAWA STASZICA W KRAKOWIE

AGH UNIVERSITY OF SCIENCE
AND TECHNOLOGY

AGH

INFLUENCE OF AMBIVALENT DOPANTS ON SCALE GROWTH THICKNESS ON METALS (HAUFFE-WAGNER THEORY)

http://home.agh.edu.pl/~grzesik

Basic literature

1. K. Hauffe, Progress in Metal Physic, **4**, 71 (1953).
2. P. Kofstad, „Nonstoichiometry, diffusion and electrical conductivity of binary metal oxides”, John Wiley, New York, 1972
3. P. Kofstad, „High-Temperature Oxidation of Metals”, John Wiley & Sons, Inc, New York-London-Sydney, 1978
4. A.S. Khanna, „Introduction to High Temperature Oxidation and Corrosion”, ASM International, Materials Park, 2002
5. S. Mrowec, „An Introduction to the Theory of Metal Oxidation”, National Bureau of Standards and the National Science Foundation, Washington, D.C., 1982
6. Z. Grzesik, ”The influence of aliovalent impurities on the sulphidation kinetics of manganese and molybdenum”, Journal of Solid State Electrochemistry, **13**, 1701-1708 (2009).
7. Z. Grzesik, "Własności transportowe zgorzelin siarczkowych powstających w procesie wysokotemperaturowej korozji metali", Ceramika, **87**, 1-124 (2005).
8. Z. Grzesik and K. Przybylski, ”Sulfidation of metallic materials”, in ”Developments in high-temperature corrosion and protection of metals”, Ed. Wei Gao and Zhengwei Li, Woodhead Publishing Limited, Cambridge, England, pp. 599-638, 2008.
9. Z. Grzesik, „Termodynamika i kinetyka defektów w kryształach jonowych”, Wydawnictwo Naukowe AKAPIT, Kraków 2011.

Hauffe-Wagner theory assumptions

- a doped scale is a single phase solid solution of dopants in the doped compound
- dopant valence is different that the valence of the cations and anions constituting the scale
- mass transport in the scale takes place through point defects
- intrinstic point defect concentration in a growing scale is very low

Reason for dopant influence on oxidation rate

According to Wagner's theory of pure metal oxidation, the oxidation rate is proportional to intrinsic defect concentration:

$$k'_p = \frac{1}{2}\int_{p'_{X_2}}^{p''_{X_2}} \left(\frac{z_c}{|z_a|} D^*_{Me} + D^*_X \right) d \ln p_{X_2}$$

$$k'_p = \left(1 + |p|\right) \cdot D^*_{Me} = [def] \cdot \tilde{D}$$

By controling the concentration of these defects, e.g. by doping, the corrosion rate can be influenced.

That same dopant, in certain cases, significantly increases, and, in other cases, decreases the metal corrosion rate. This phenomenon is illustrated in a subsequent part of the presentation using the example of doping manganese and molybdenium – two metals that form scales with unusally low defect concentration ($y < 10^{-3}$).

α-MnS sulfide properties

- NaCl crystalline structure
- metal deficient p-type semiconductor, $Mn_{1-y}S$
- low point defect concentration $\left(V''_{Mn}; h^{\bullet}\right)$

$y < 10^{-3}$ w T = 1273 K i $p(S_2) = 10^4$ Pa

α-MnS sulfide properties, cont.

$$\frac{1}{2}S_2 \Leftrightarrow V''_{Mn} + 2h^{\bullet} + S_S$$

$$\left[V''_{Mn}\right] = \tfrac{1}{2}\left[h^{\bullet}\right] = 0.63 \cdot p_{S_2}^{1/6} \cdot \exp\left(\frac{\frac{1}{3}\Delta S_f}{R}\right) \cdot \exp\left(-\frac{\frac{1}{3}\Delta H_f}{RT}\right)$$

$$y = \left[V''_{Mn}\right] = \tfrac{1}{2}\left[h^{\bullet}\right] = 4.77 \cdot 10^{-2} \cdot p_{S_2}^{1/6} \cdot \exp\left(-\frac{41.5\,kJ/mol}{RT}\right)$$

$$D_V = 1.97 \cdot 10^{-2} \cdot \exp\left(-\frac{83.4\,kJ/mol}{RT}\right)$$

Manganese sulphidation rate

theoretical deliberations:

$$k'_p = 3\,D_V\left[V''_{Mn}\right] = 2.82\cdot 10^{-3}\; p_{S_2}^{1/6} \exp\left(-\frac{124.9\ \text{kJ/mol}}{RT}\right)$$

experimental results:

$$k'_p = 3.51\cdot 10^{-3}\, p_{S_2}^{1/6} \exp\left(-\frac{127\,\text{kJ}/\text{mol}}{RT}\right)$$

SEM picture of the surface and cross-section of a sulfide scale formed on manganese

(1000 °C, $p(S_2) = 10^3$ Pa, 240 h)

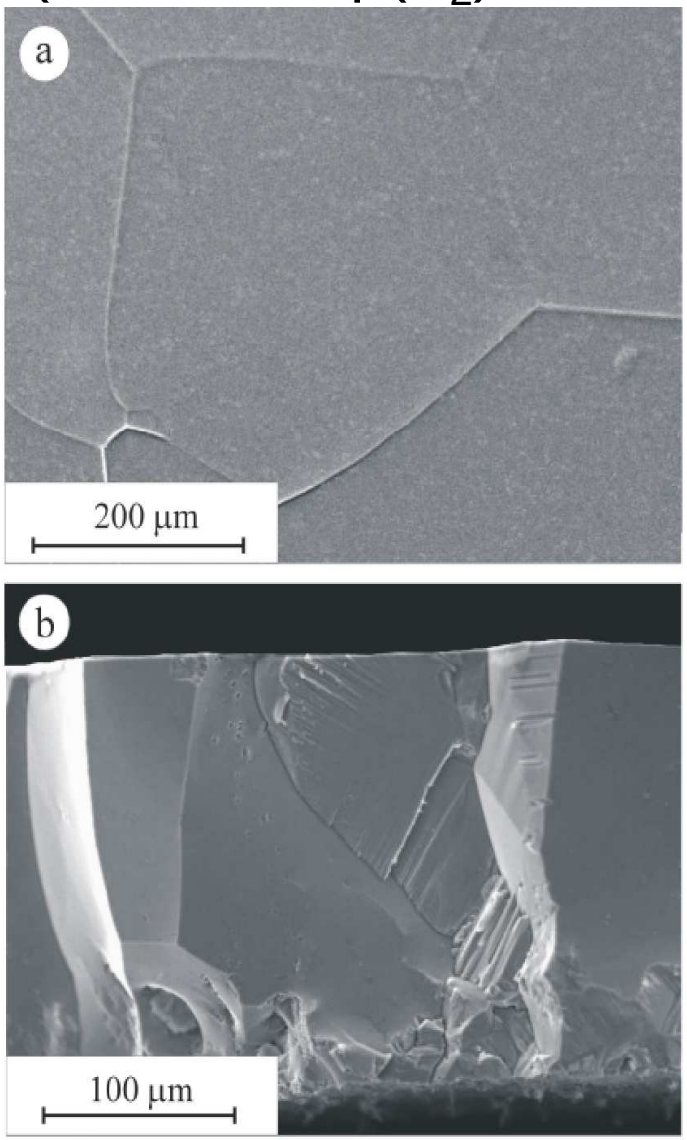

surface

fracture

Defect concentration in a $Mn_{1-y}S$-Cr_2S_3 solid solution

$$Cr_2S_3 \Leftrightarrow 2Cr_{Mn}^{\bullet} + V_{Mn}'' + 3S_S$$

$$Cr_2S_3 + 2h^{\bullet} \Leftrightarrow 2Cr_{Mn}^{\bullet} + 2S_S + \frac{1}{2}S_2$$

$$\left[Cr_{Mn}^{\bullet}\right] + \left[h^{\bullet}\right] = 2\left[V_{Mn}''\right]$$

Gdy $\left[Cr_{Mn}^{\bullet}\right] >> \left[h^{\bullet}\right]$, to $\left[Cr_{Mn}^{\bullet}\right] = 2\left[V_{Mn}''\right]$

Pressure dependence of the parabolic rate constant of Mn-5%Cr alloy sulphidation, on the background of analogous data obtained for Mn

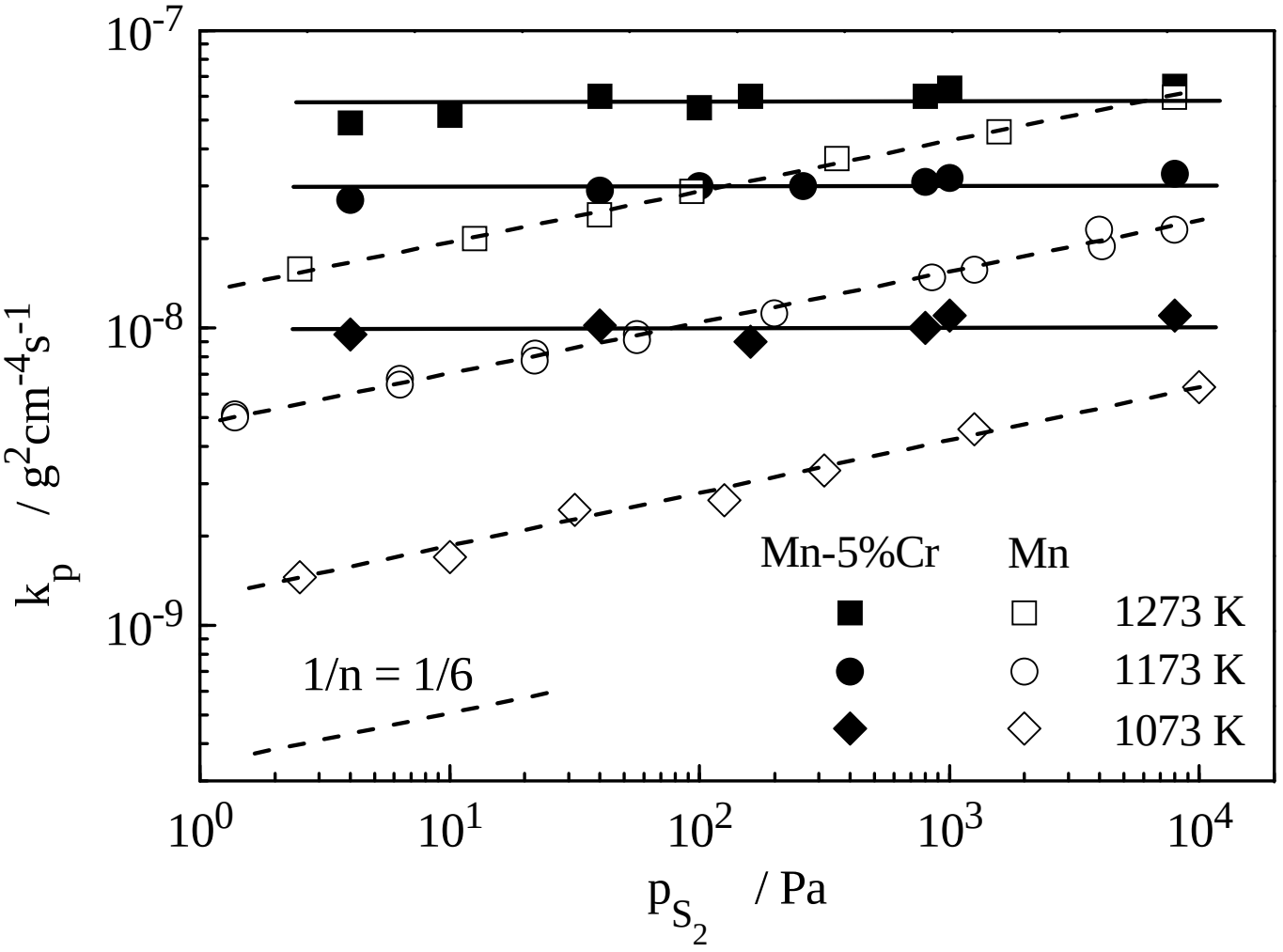

Defect concentration in a $Mn_{1-y}S$-Li_2S solid solution

$$Li_2S + V''_{Mn} = 2\,Li'_{Mn} + S_S$$

$$Li_2S + \tfrac{1}{2}S_2 = 2\,Li'_{Mn} + 2\,h^{\bullet} + 2\,S_S$$

$$\left[Li'_{Mn}\right] + 2\left[V''_{Mn}\right] = \left[h^{\bullet}\right]$$

Gdy $\left[Li'_{Mn}\right] >> \left[V''_{Mn}\right]$, to $\left[Li'_{Mn}\right] = \left[h^{\bullet}\right]$

$$\left[V''_{Mn}\right] = \frac{1}{\left[Li'_{Mn}\right]^2} \cdot p_{S_2}^{1/2} \cdot \exp\left(\frac{\Delta S_f}{R}\right) \cdot \exp\left(-\frac{\Delta H_f}{RT}\right)$$

Influence of Li dopant on ionic defect concentration in $Mn_{1-y}S$

Mn-Li:

$$\left[V''_{Mn}\right] = \frac{1}{\left[Li'_{Mn}\right]} \cdot p_{S_2}^{1/2} \cdot \exp\left(\frac{\Delta S_f}{R}\right) \cdot \exp\left(-\frac{\Delta H_f}{RT}\right)$$

$$E'_D = \Delta H_f + \Delta H_m = 207{,}9\ \mathrm{kJ/mol}$$

Mn:

$$\left[V''_{Mn}\right] = 0{,}63 \cdot p_{S_2}^{1/6} \cdot \exp\left(\frac{\frac{1}{3}\Delta S_f}{R}\right) \exp\left(-\frac{\frac{1}{3}\Delta H_f}{RT}\right)$$

$$E_D = \frac{1}{3}\Delta H_f + \Delta H_m = 124{,}4\ \mathrm{kJ/mol}$$

Schematic illustration of an apparatus for sulphidation in Li_2S-containing atmosphere

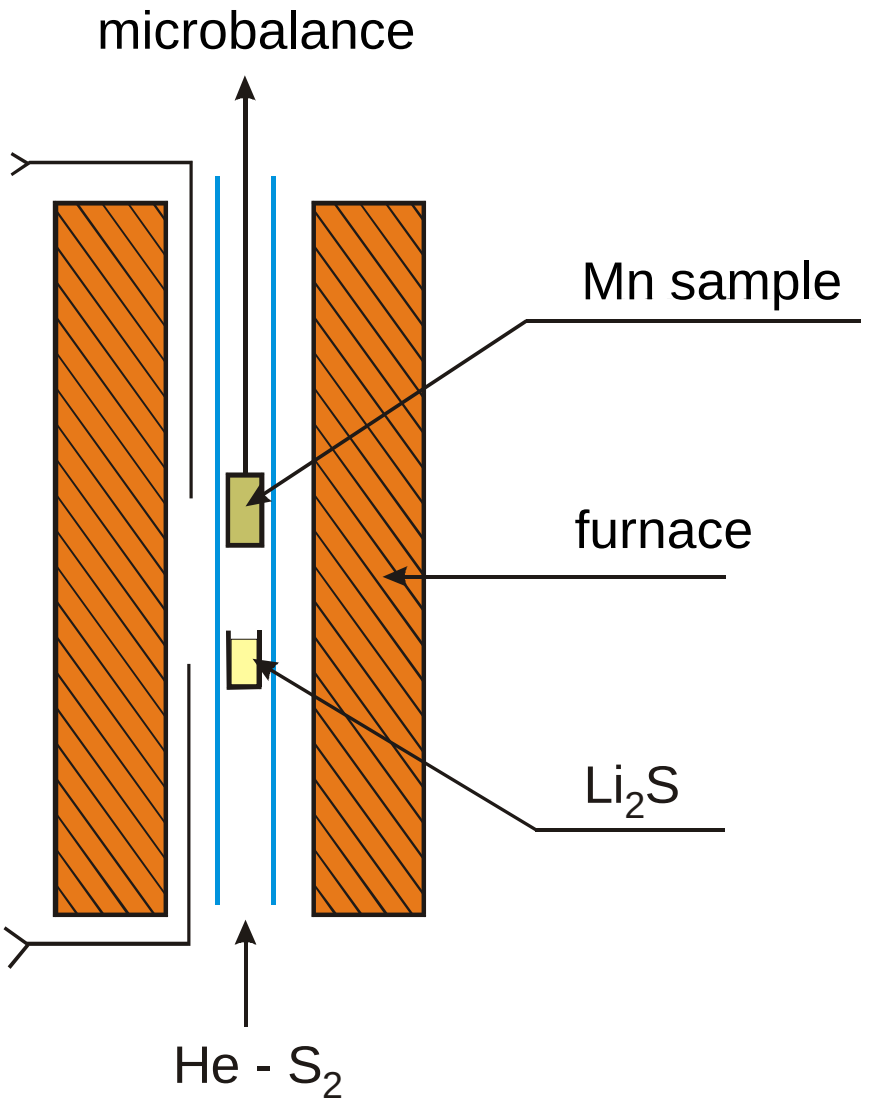

Correlation between k_p and pressure for pure and Li-doped Mn

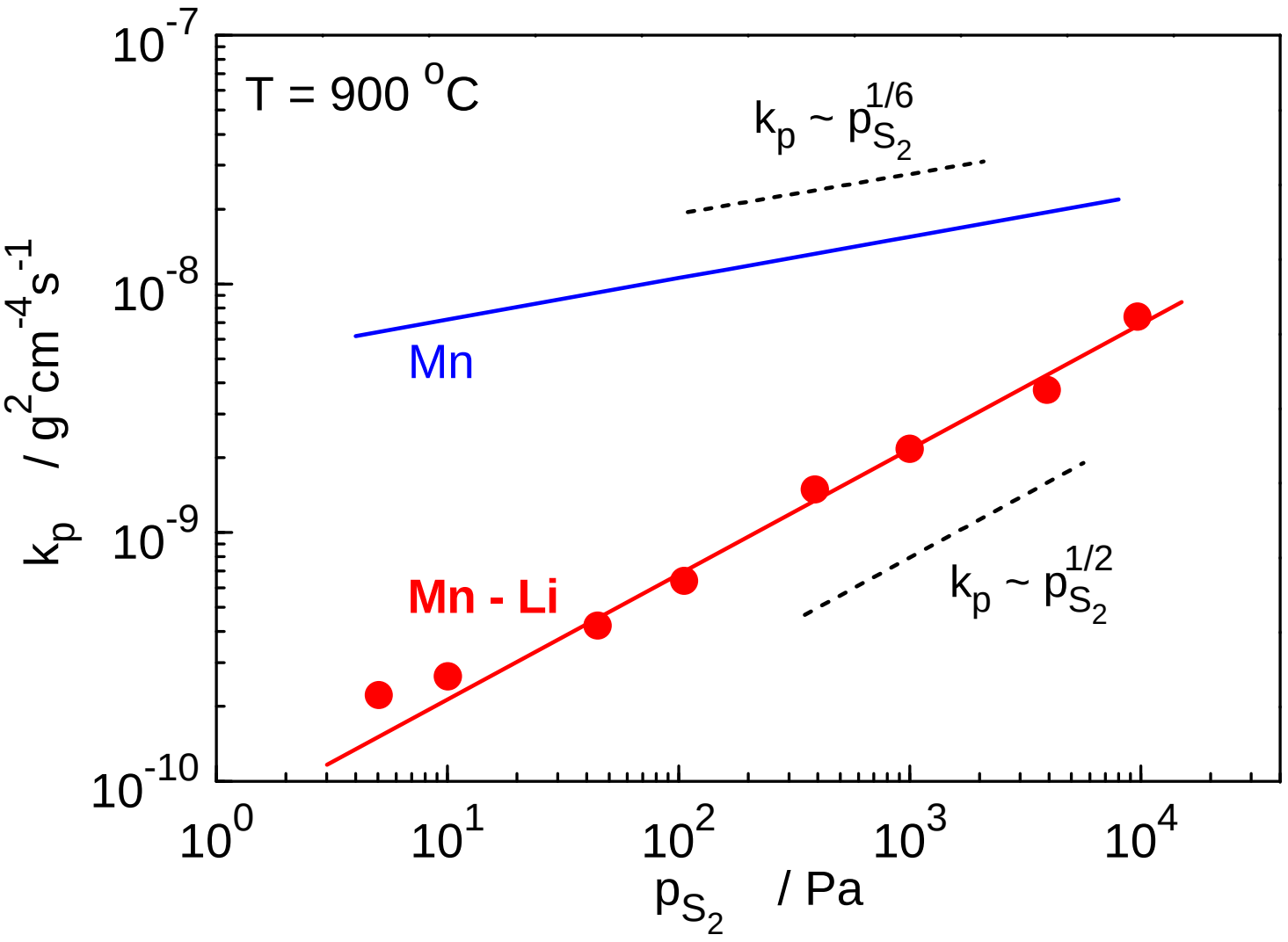

Correlation between k_p and temperature for pure and Li-doped Mn

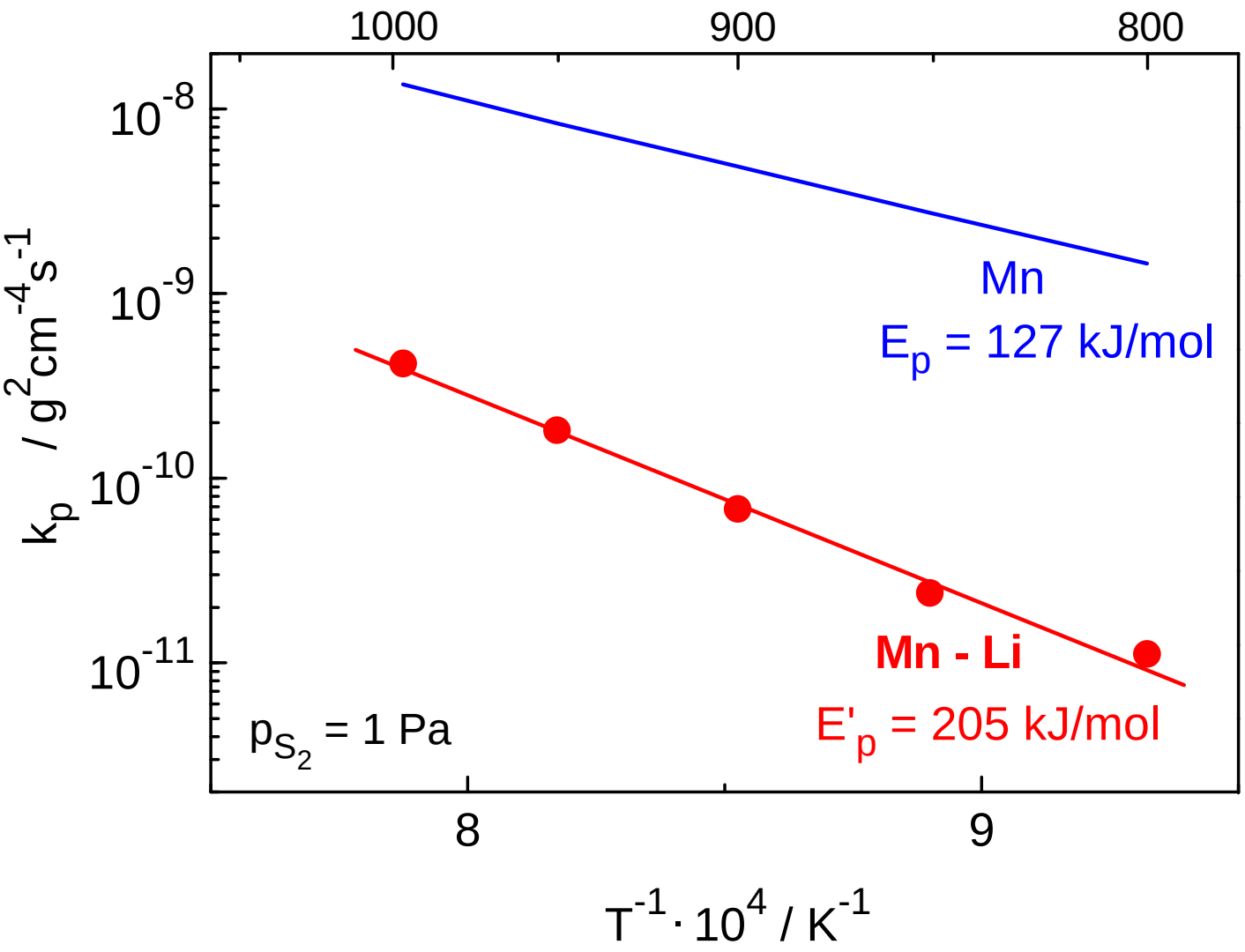

Pressure dependence of the parabolic rate constant of Mn sulphidation in pure and Li_2S-containing sulfur vapors

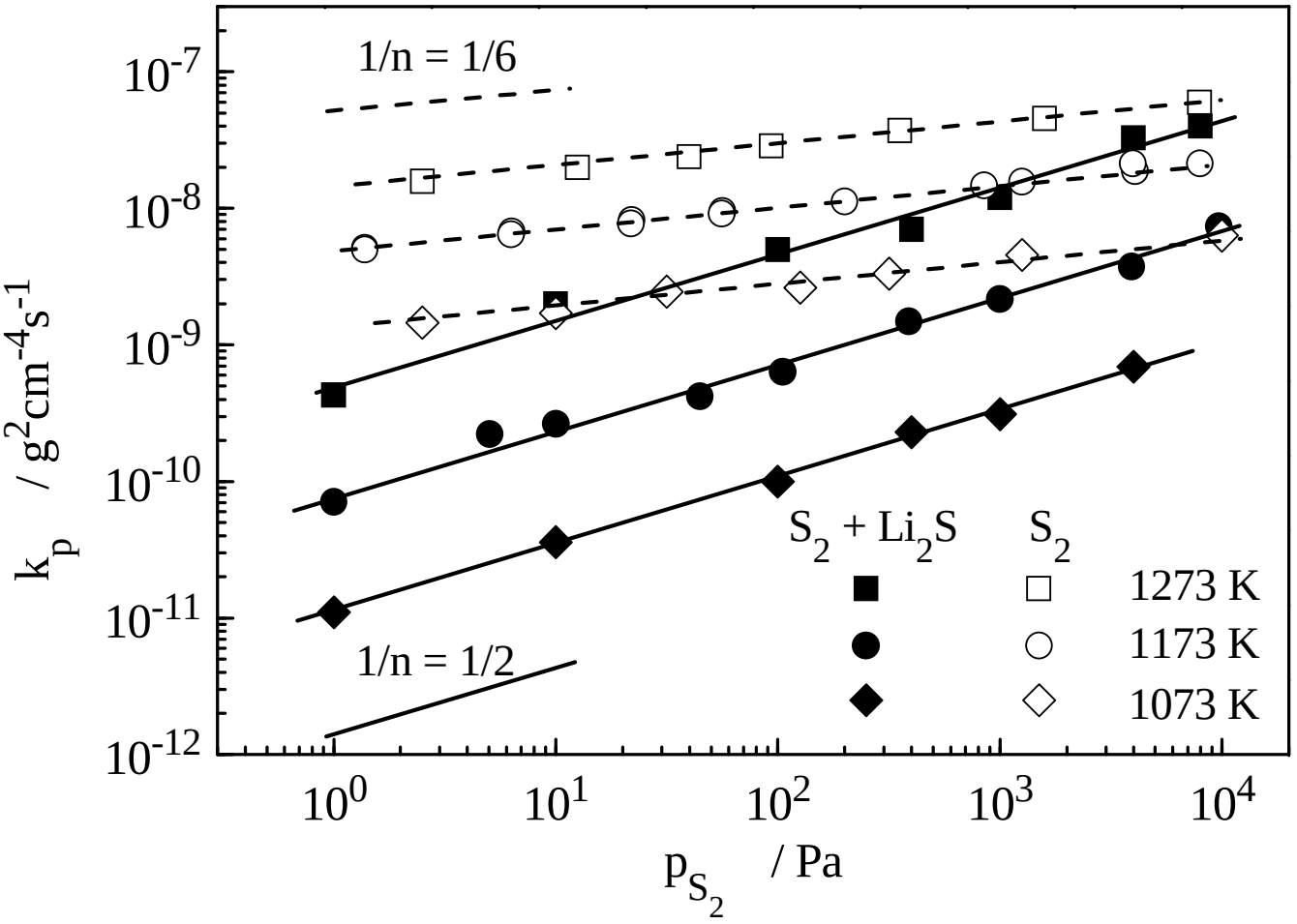

Correlation between k_p and temperautre for several metals

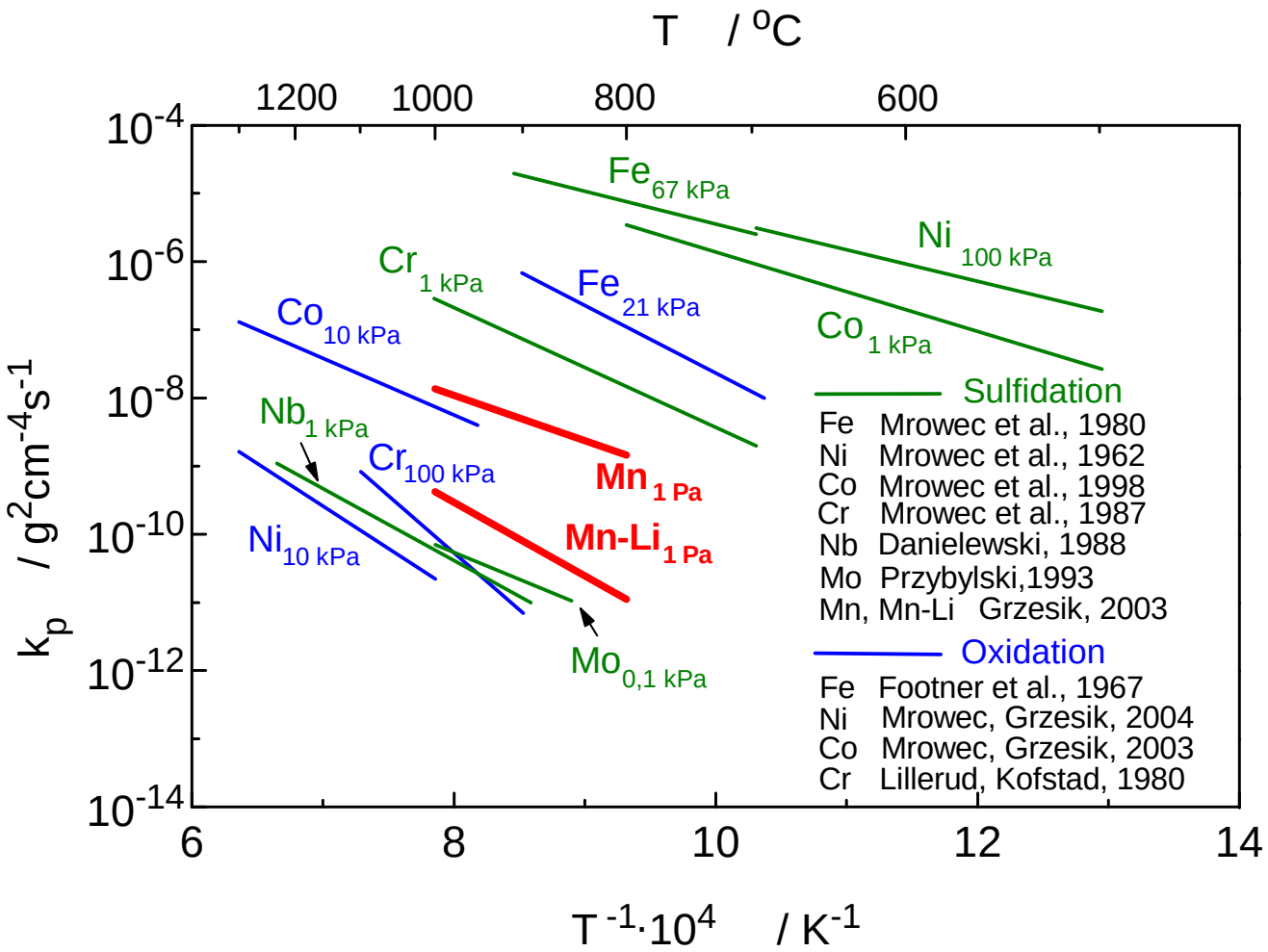

MoS_2 sulfide properties

$$\frac{1}{2}S_2 \Leftrightarrow S_i'' + 2h^{\bullet}$$

$$\text{zero} \Leftrightarrow h^{\bullet} + e'$$

$$2[S_i''] + [e'] = [h^{\bullet}]$$

Gdy $[e'] = [h^{\bullet}]$, to $[S_i''] = \text{const} \cdot p_{S_2}^{1/2}$

Defect concentration in a MoS_2-Cr_2S_3 solid solution

$$Cr_2S_3 + S_i'' \Leftrightarrow 2Cr_{Mo}' + 4S_S$$

$$Cr_2S_3 + \tfrac{1}{2}S_2 \Leftrightarrow 2Cr_{Mo}' + 2h^{\bullet} + 4S_S$$

$$\left[Cr_{Mo}'\right] + \left[e'\right] + 2\left[S_i''\right] = \left[h^{\bullet}\right]$$

Gdy $\left[Cr_{Mo}'\right] = \left[h^{\bullet}\right]$, to $\left[S_i''\right] = \text{const} \cdot \left[Cr_{Mo}'\right]^{-2} \cdot p_{S_2}^{1/2}$

Temperature dependence of Mo-Cr alloy sulphidation rate on the background of an analogous dependence obtained for pure molybdenium

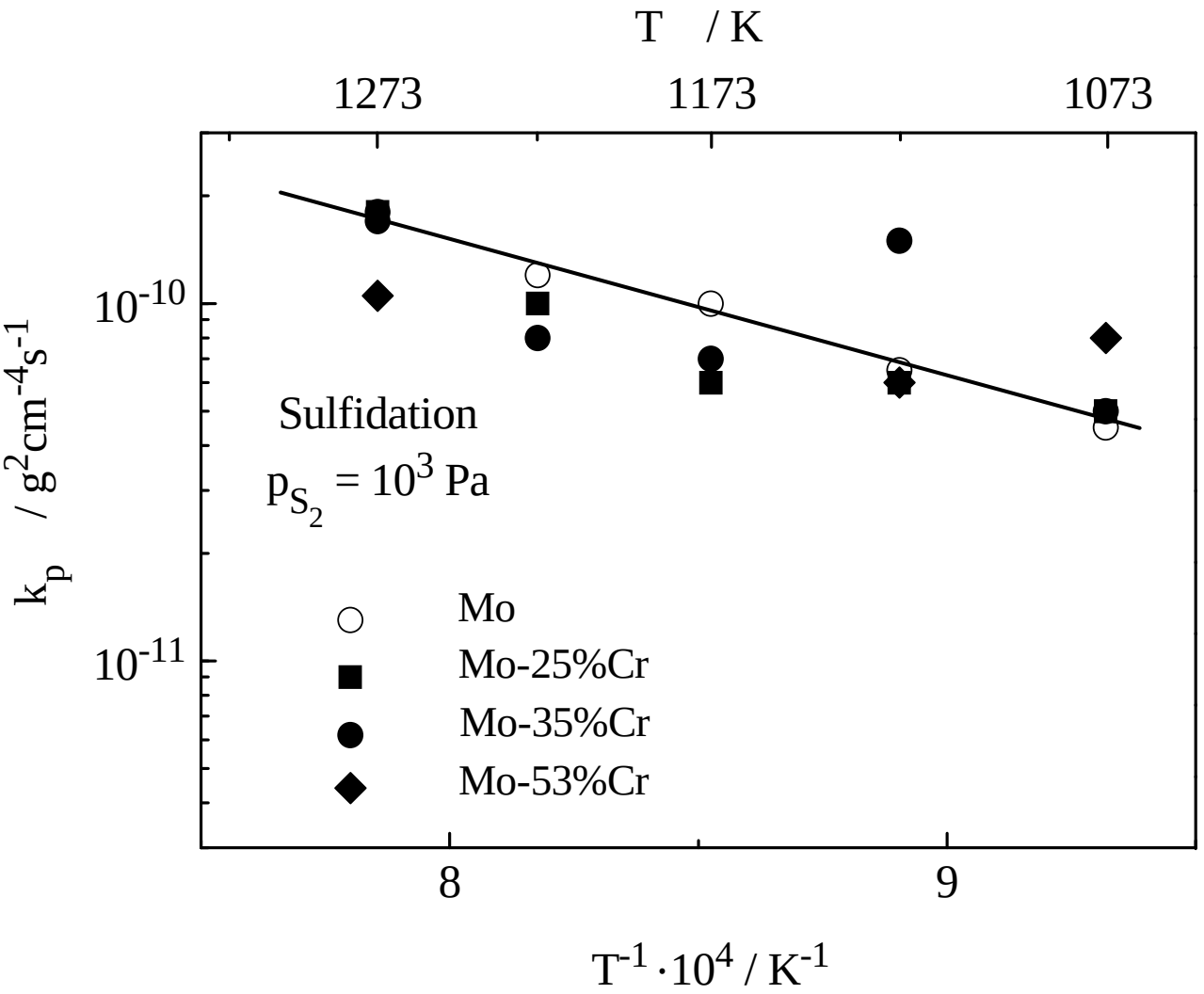

Defect concentration in a MoS_2-Li_2S solid solution

$$Li_2S + 3S_i'' \Leftrightarrow 2Li_{Mo}''' + 4S_S$$

$$Li_2S + \tfrac{3}{2}S_2 \Leftrightarrow 2Li_{Mo}''' + 6h^{\bullet} + 4S_S$$

$$3\left[Li_{Mo}'''\right] + \left[e'\right] + 2\left[S_i''\right] = \left[h^{\bullet}\right]$$

Gdy $\left[Li_{Mo}'''\right] = \left[h^{\bullet}\right]$, to $\left[S_i''\right] = \text{const} \cdot \left[Li_{Mo}'''\right]^{-2} \cdot p_{S_2}^{1/2}$

Pressure dependence of the parabolic rate constant of molybdenium sulphidation in pure and Li_2S-containing sulfur vapors

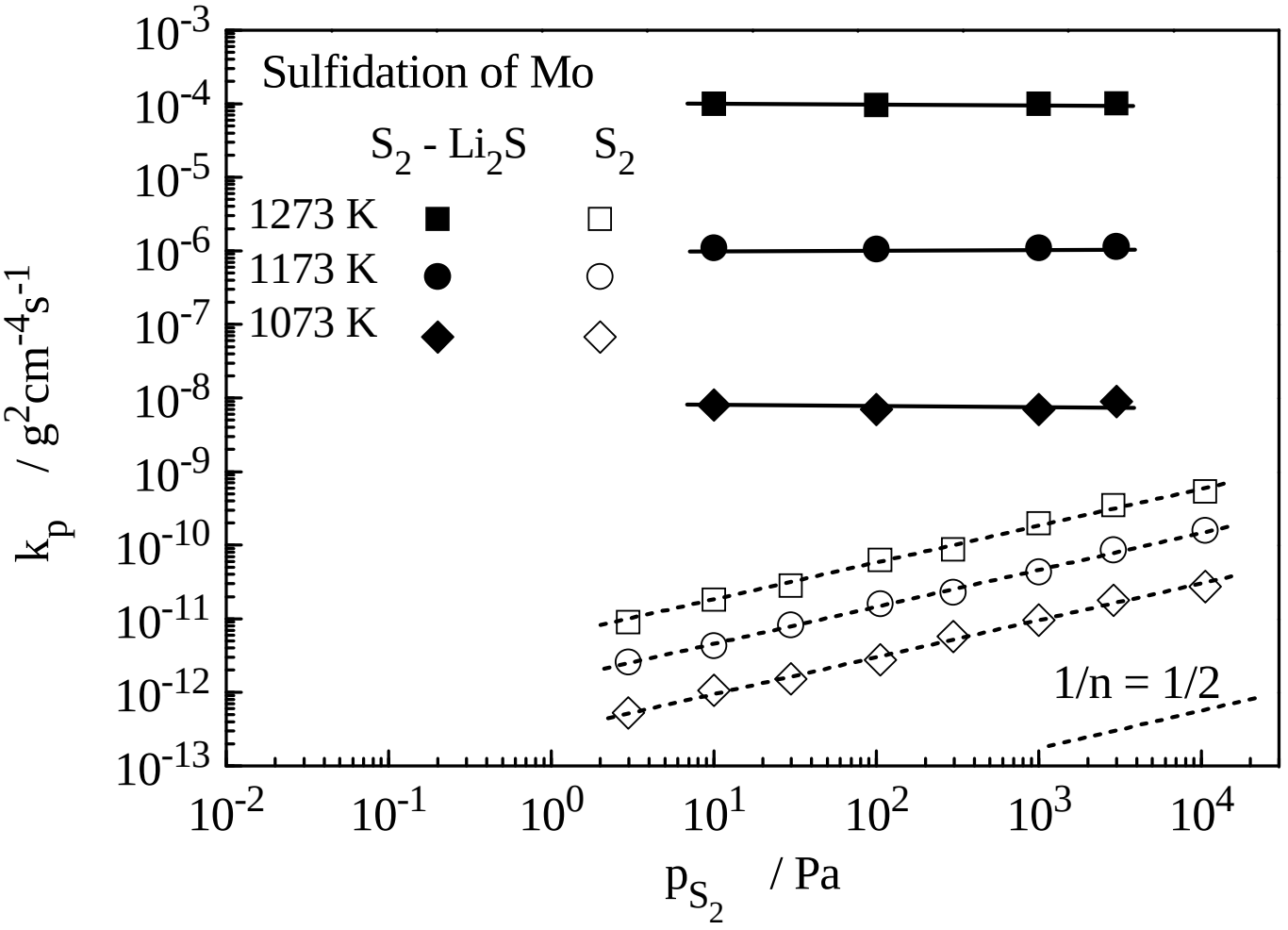

Defect concentration in a MoS_2-Li_2S solid solution, assuming that lithium inserts itself into the MoS_2 crystalline lattice interstitially

$$Li_2S = 2\,Li_i^{\bullet} + S_i''$$

$$\left[S_i''\right] = \frac{1}{2}\left[Li_i^{\bullet}\right]$$

Pressure dependence of the parabolic rate constant of molybdenium sulphidation in pure and Li_2S-containing sulfur vapors

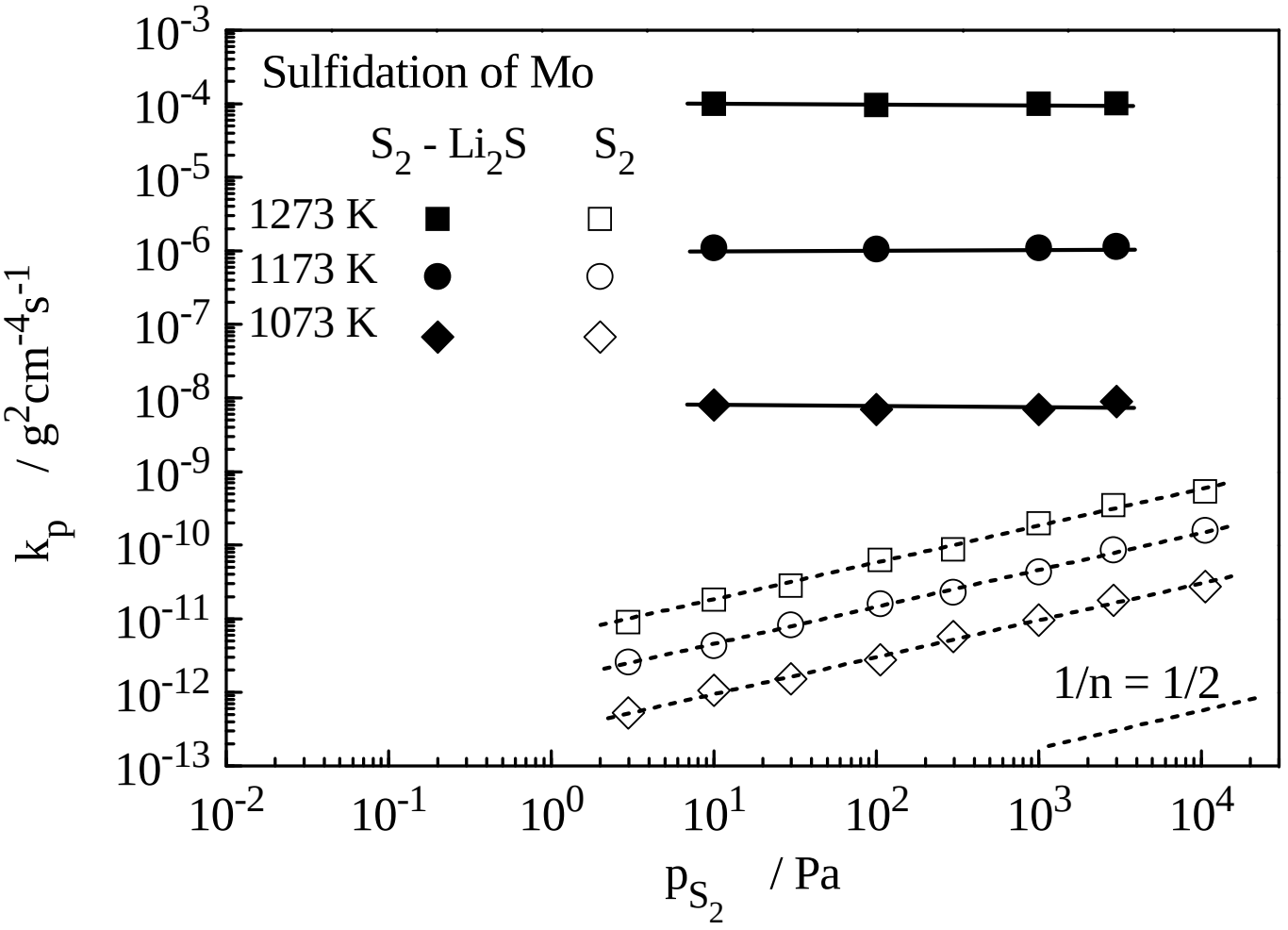

Conclusion

The same dopant (in the disscussed case of lithium) in certain compounds can significantly increase, and in others decrease the metal corrosion rate. Unfortunately, it is not possible to *a priori* forsee the influence of the dopant on the metal corrosion kinetics on the basis of Hauffe and Wagner's doping theory, if the way the dopant incorporates itself into a given lattice is not known.

Influence of chromium doping on the cobalt oxidation rate

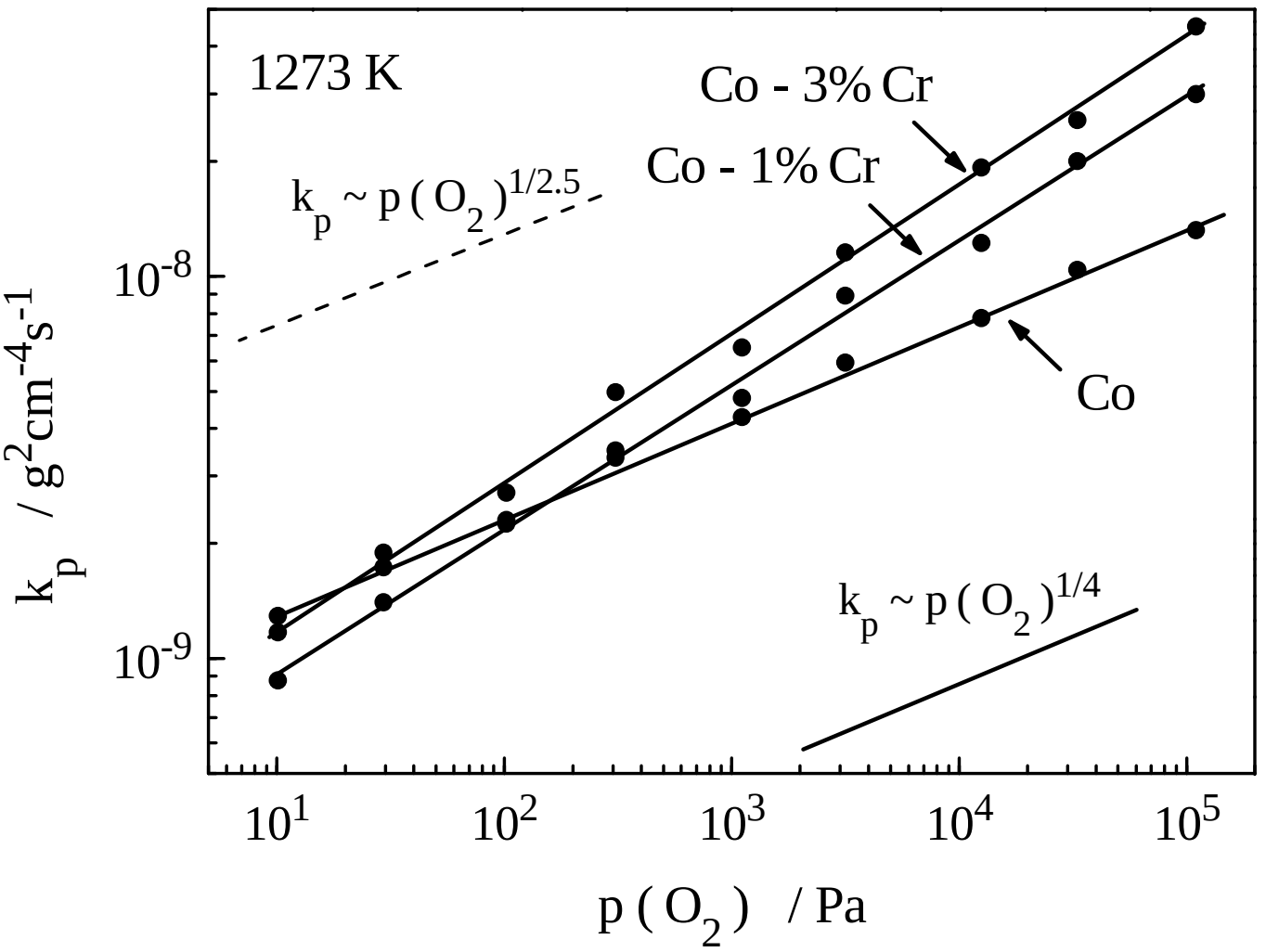

S. Mrowec and Z. Grzesik, Journal of Physics and Chemistry of Solids, 64, 1387-1394 (2003)

Influence of chromium doping on deviation from stoichiometry in $Co_{1-y}O$

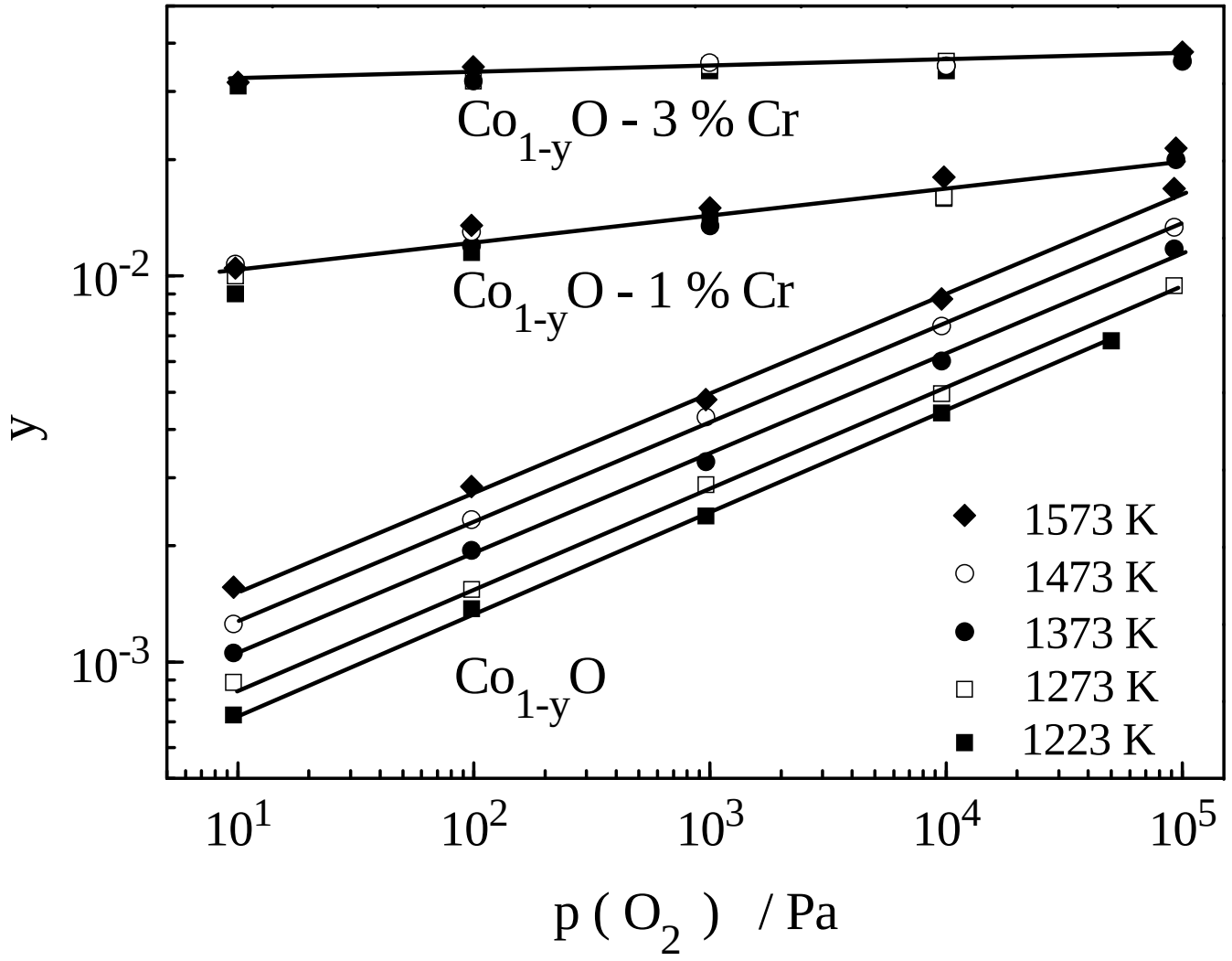

S. Mrowec and Z. Grzesik, Journal of Physics and Chemistry of Solids, 64, 1387-1394 (2003)

Summary of the chromium dopant influence on Co-Cr alloy oxidation rates and deviation from stoichiometry in $Co_{1-y}O$

The different characteristics of pressure dependence of Co-Cr alloy oxidation rates and deviation from stoichiometry in $Co_{1-y}O$ doped with chromium suggests that the dopants not only influence the concentration of defects, but also their mobility.

$$k'_p = \left(1 + |p|\right) \cdot D^*_{Me} = [def] \cdot \tilde{D}$$

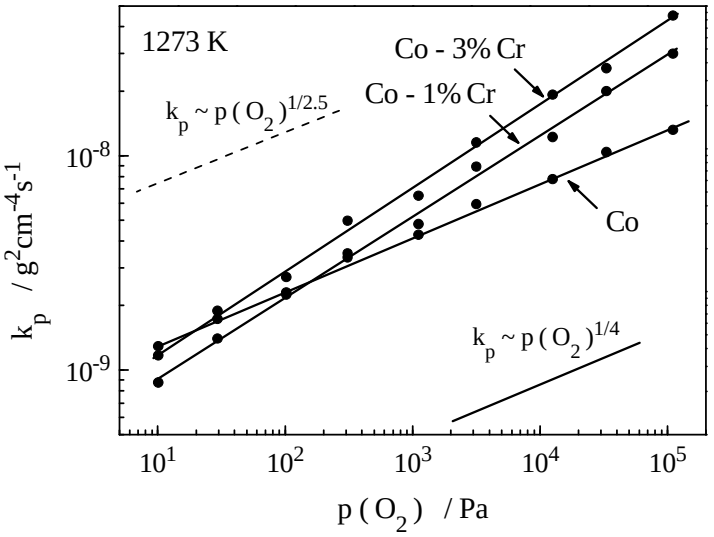

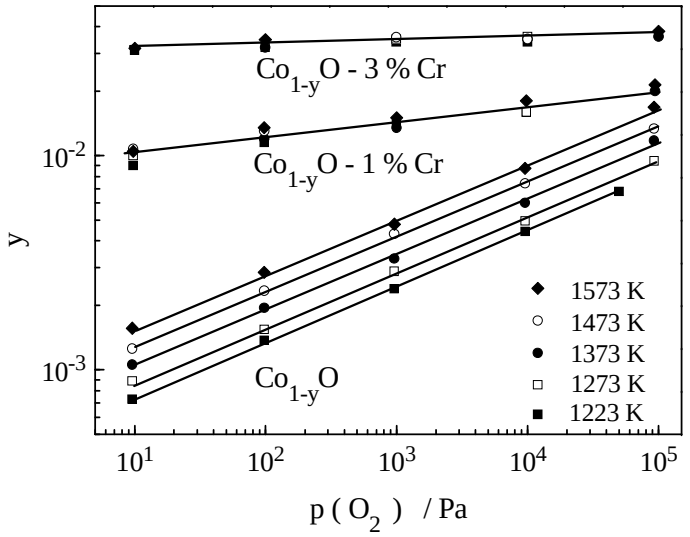

Reequilibration kinetics of $Co_{1-y}O$ and $Co_{1-y}O$-Cr_2O_3

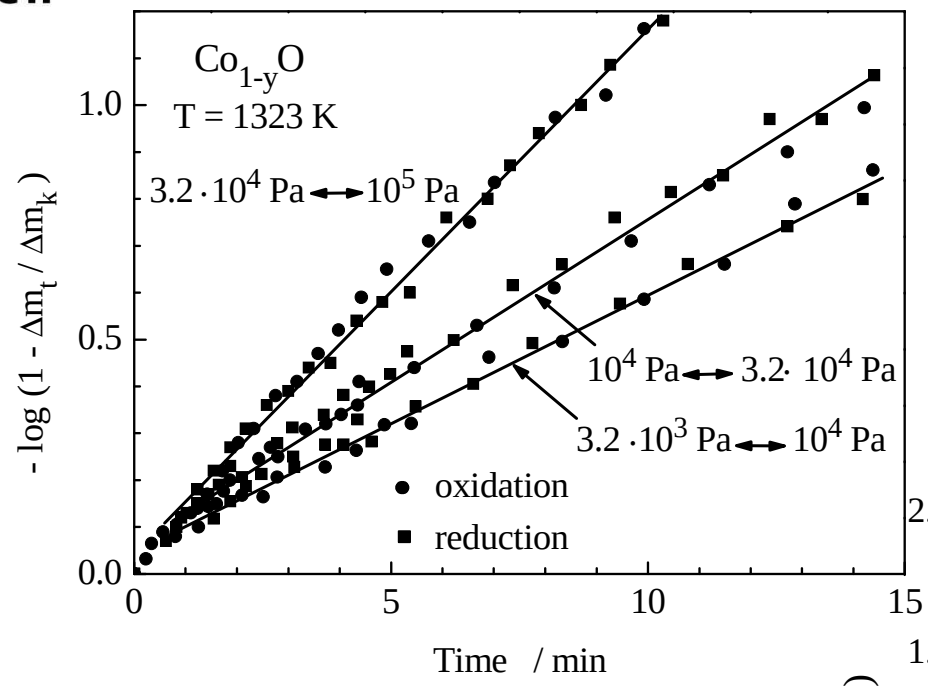

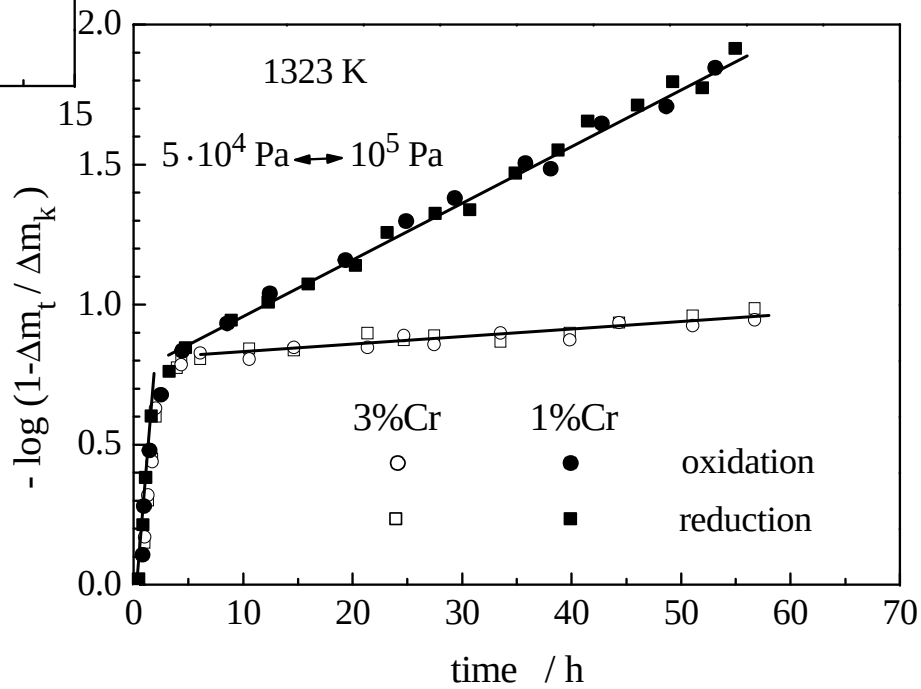

S. Mrowec and Z. Grzesik, Journal of Physics and Chemistry of Solids, 64, 1387-1394 (2003)

Influence of the chromium dopant on the chemical diffusion of defects in $Co_{1-y}O$

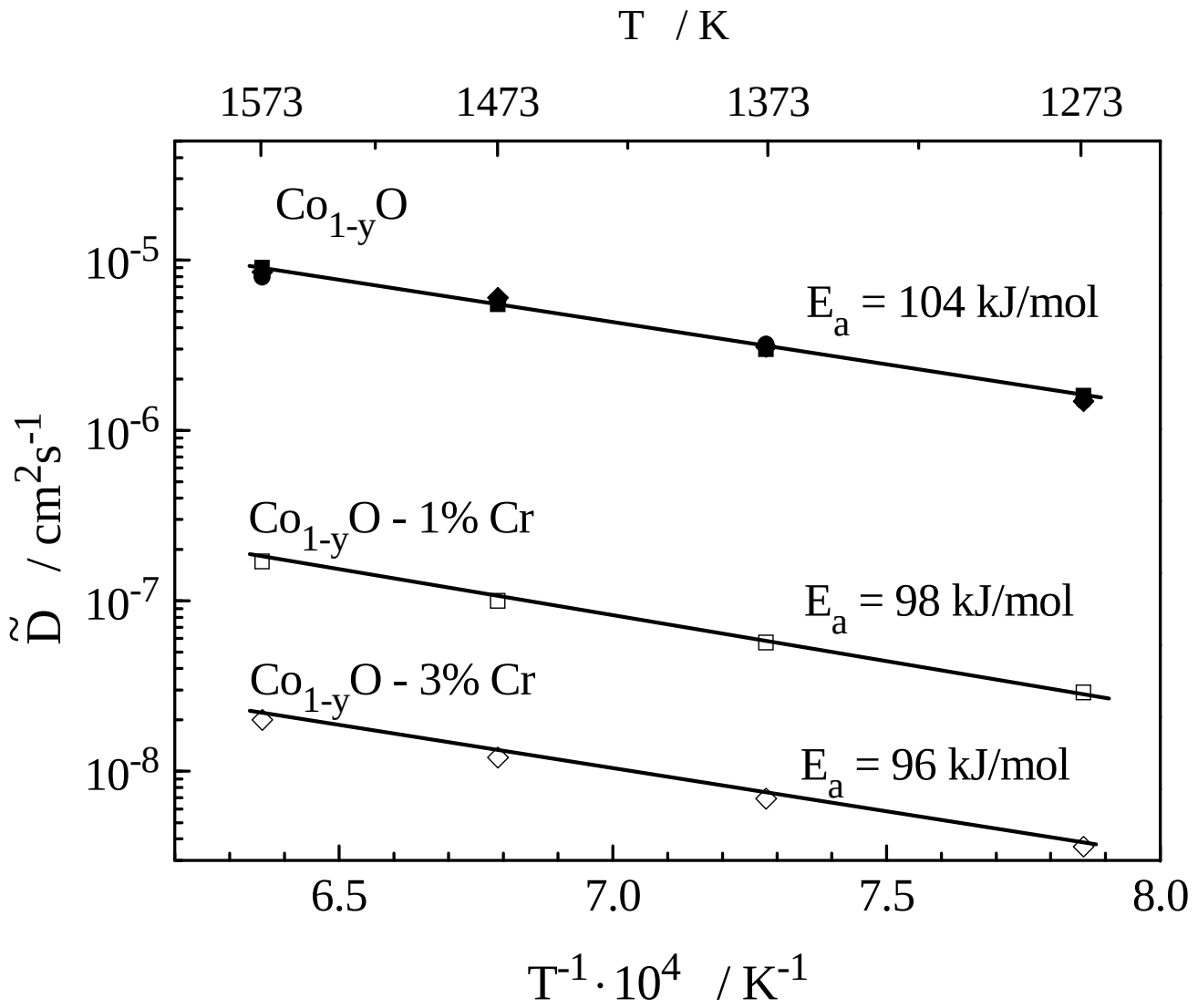

S. Mrowec and Z. Grzesik, Journal of Physics and Chemistry of Solids, 64, 1387-1394 (2003)

Influence of lithium and aluminum on oxidation kinetics of zinc at 673 K

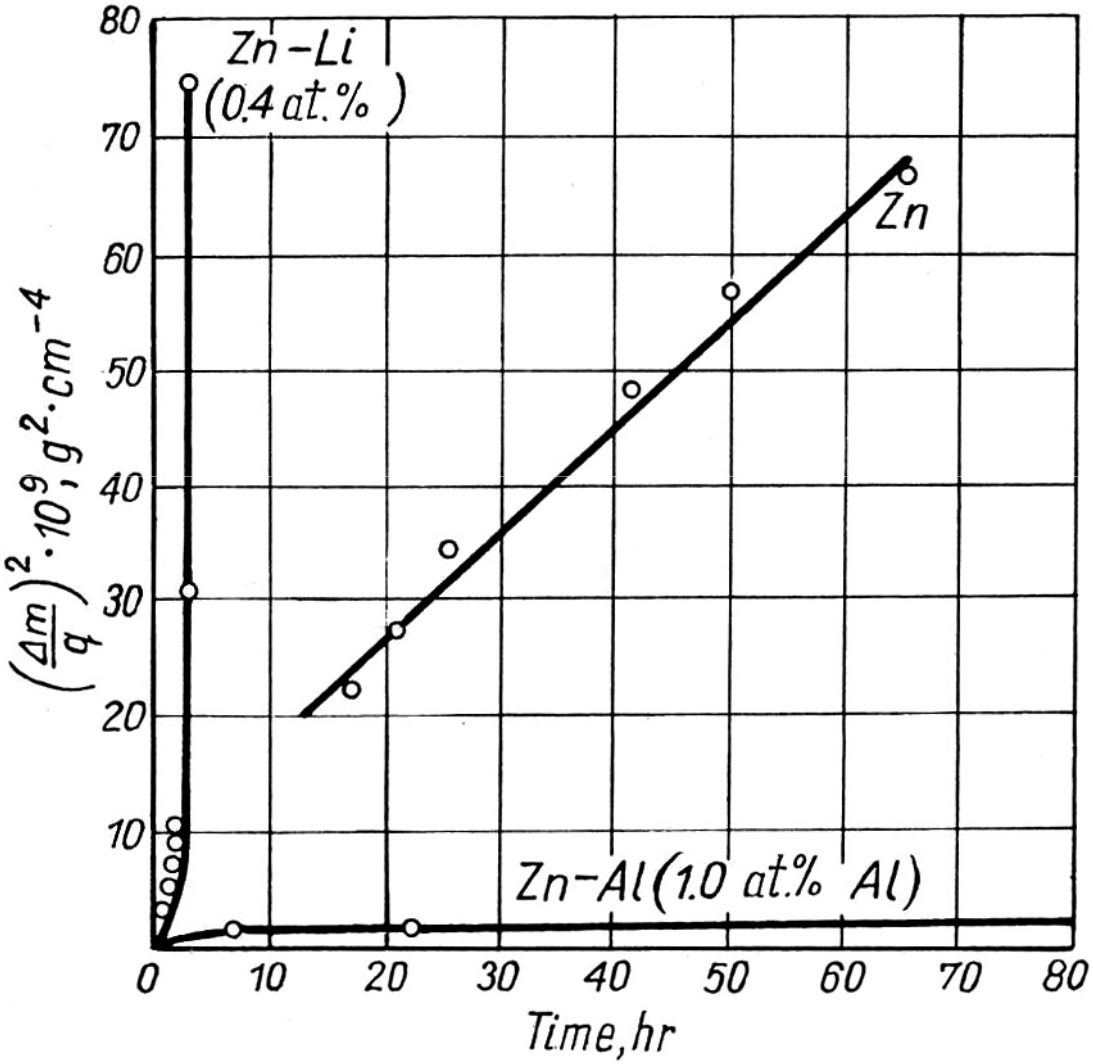

S. Mrowec, „An Introduction to the Theory of Metal Oxidation”, National Bureau of Standards and the National Science Foundation, Washington, D.C., 1982

Influence of chromium and manganese on nickel oxiation kinetics at 1173 K

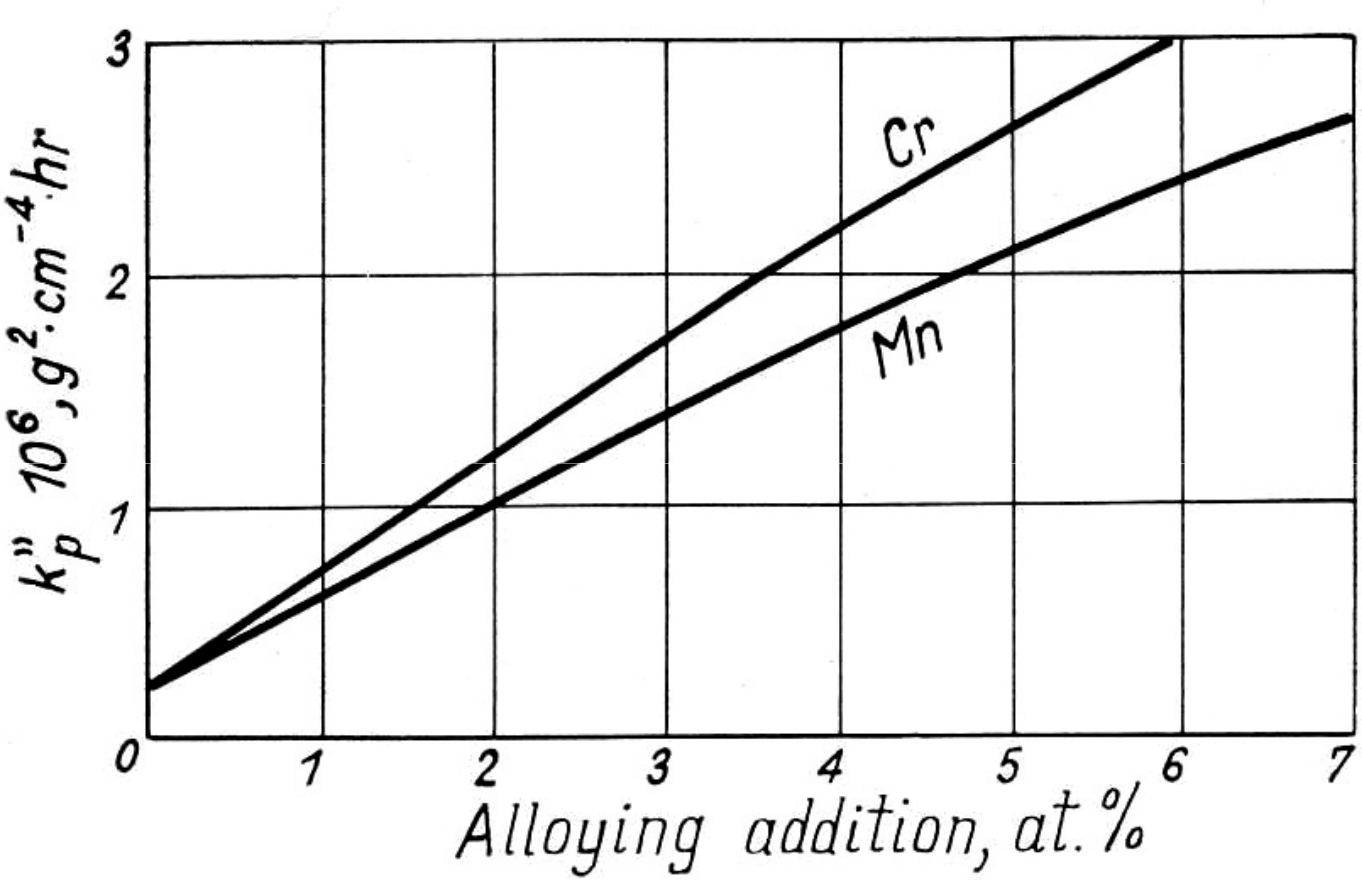

Note: high alloying element concentration does not denote that its concentration in the NiO crystalline lattice is just as high.

S. Mrowec, „An Introduction to the Theory of Metal Oxidation”, National Bureau of Standards and the National Science Foundation, Washington, D.C., 1982

Lithium influence, as an alloying element, on nickel oxidaiton kinetics at 1473 K

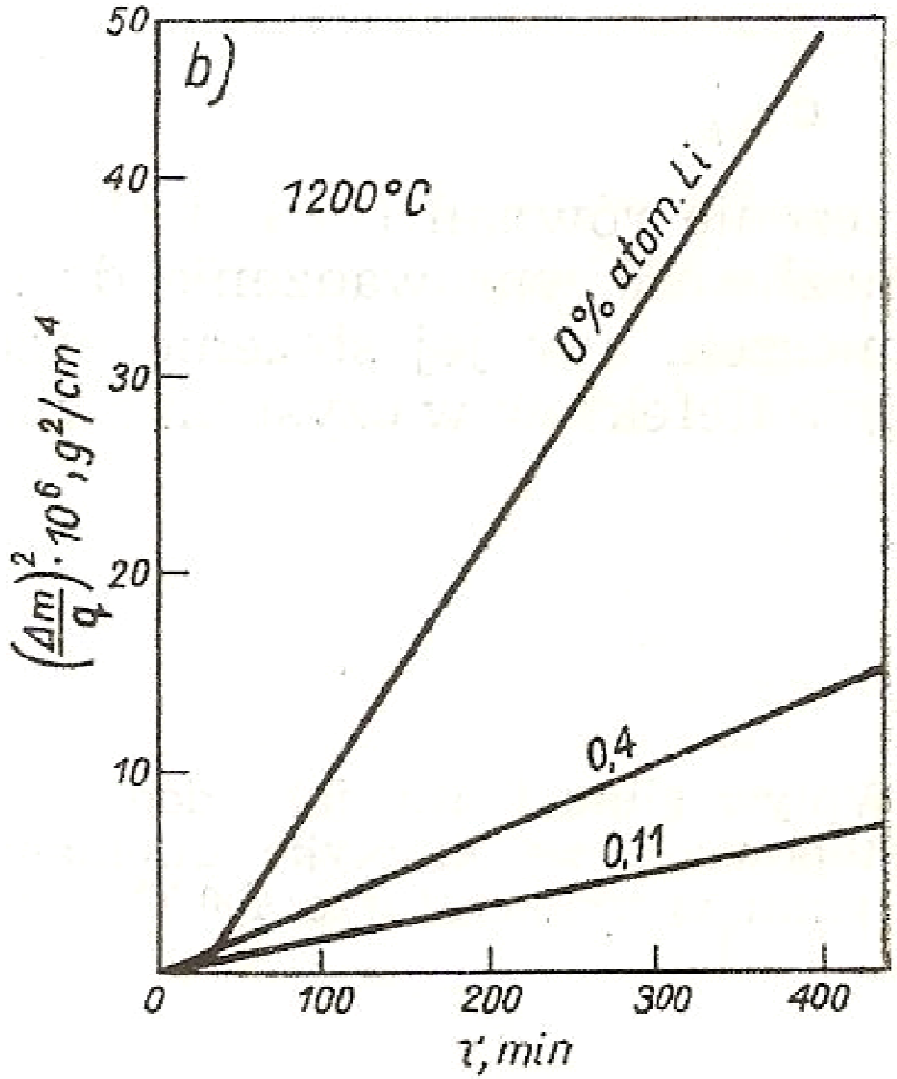

S. Mrowec, „An Introduction to the Theory of Metal Oxidation”, National Bureau of Standards and the National Science Foundation, Washington, D.C., 1982

Comparison between nickel oxidation kinetics (1) and kinetics obtained during oxidation in a Li_2O vapor-containing atmosphere (2)

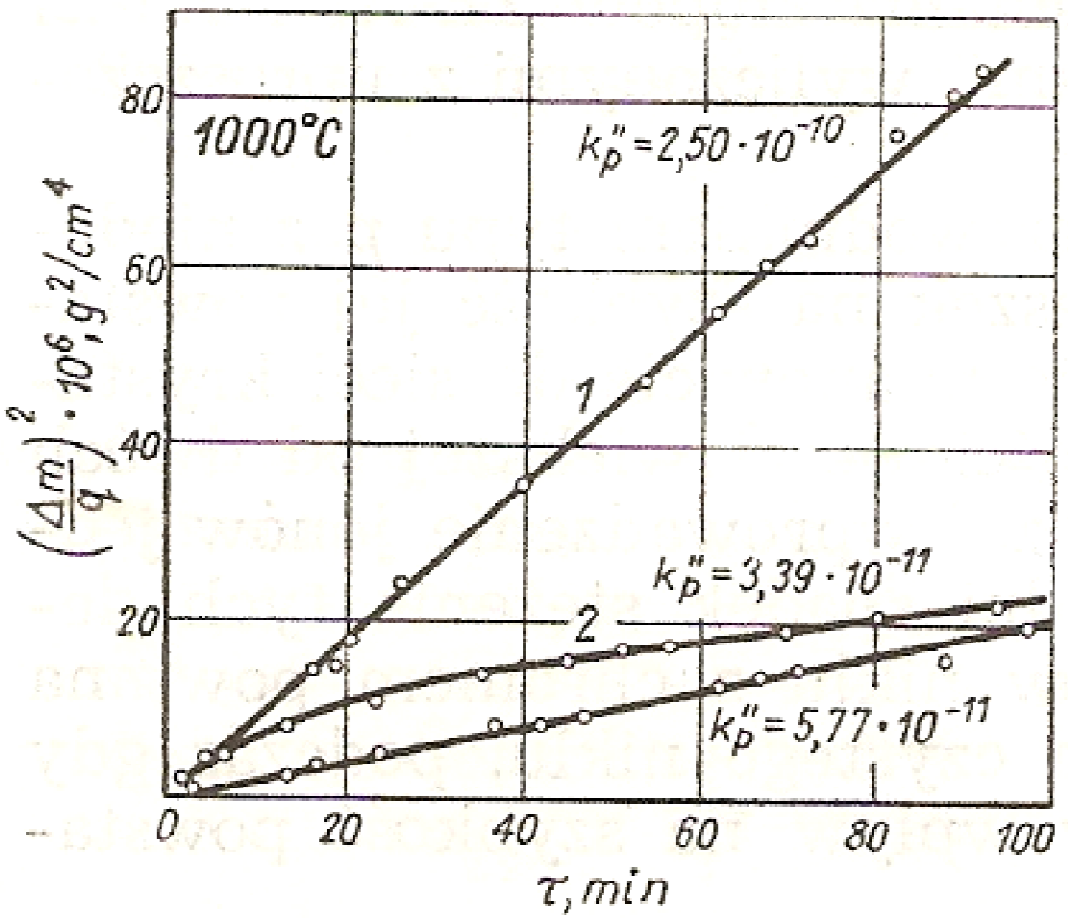

S. Mrowec, „An Introduction to the Theory of Metal Oxidation”, National Bureau of Standards and the National Science Foundation, Washington, D.C., 1982

Influence of nitrogen presence (a) and WO_3 (b) in an oxidizing atmosphere on titanium oxidation kinetics

$$N_2 \leftrightarrow 2N'_O + V_O^{\bullet\bullet}$$

$$WO_3 \leftrightarrow W_{Ti}^{\bullet\bullet} - V_O^{\bullet\bullet} + 3O_O^x$$

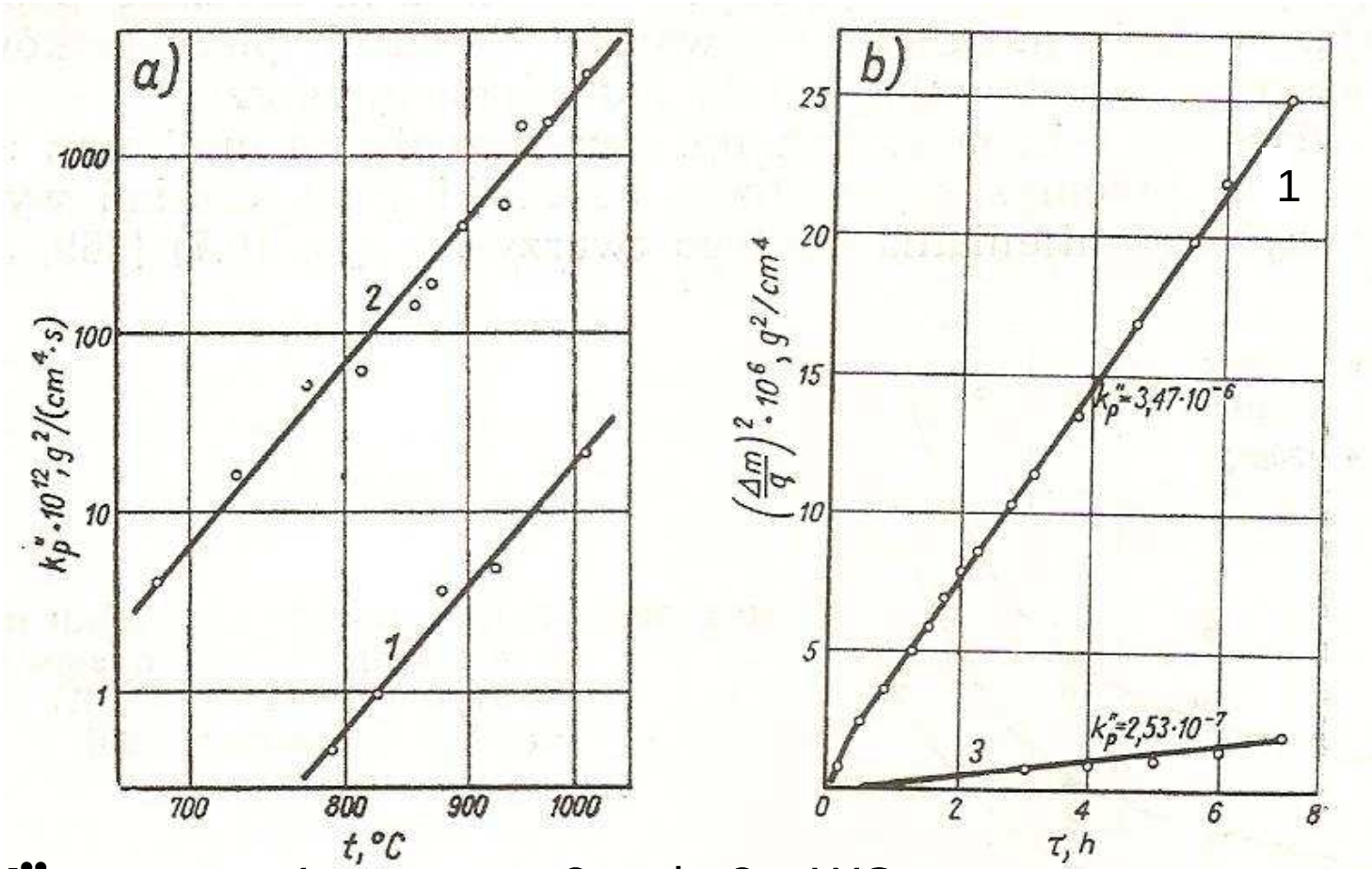

TiO_2: $V_O^{\bullet\bullet}$

1 – oxygen; 2 – air; 3 – WO_3

S. Mrowec, „An Introduction to the Theory of Metal Oxidation”, National Bureau of Standards and the National Science Foundation, Washington, D.C., 1982

Influence of the chromium dopant on iron oxidation kinetics

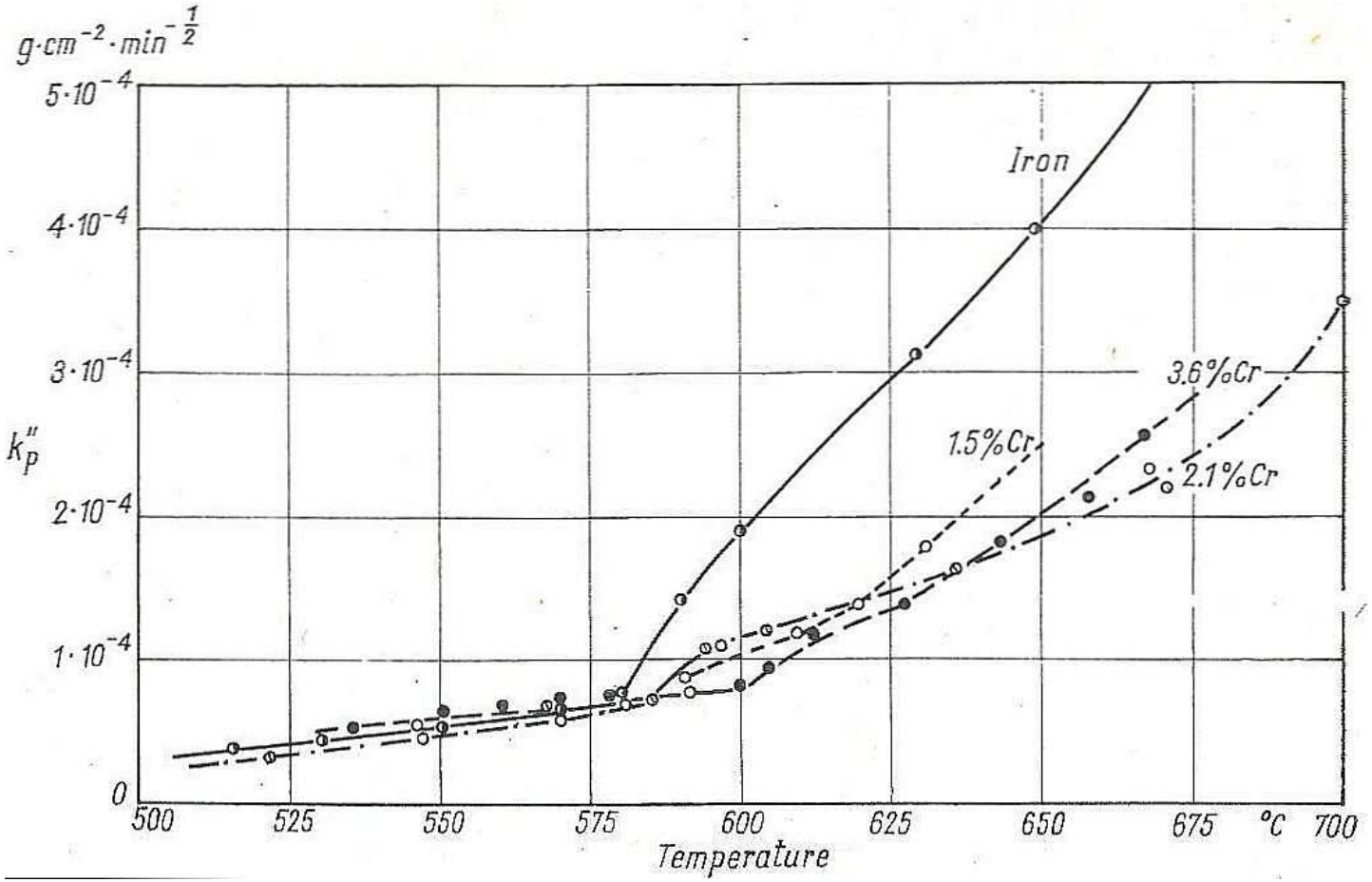

S. Mrowec, „An Introduction to the Theory of Metal Oxidation”, National Bureau of Standards and the National Science Foundation, Washington, D.C., 1982

Influence of the nickel dopant on iron oxidation kinetics

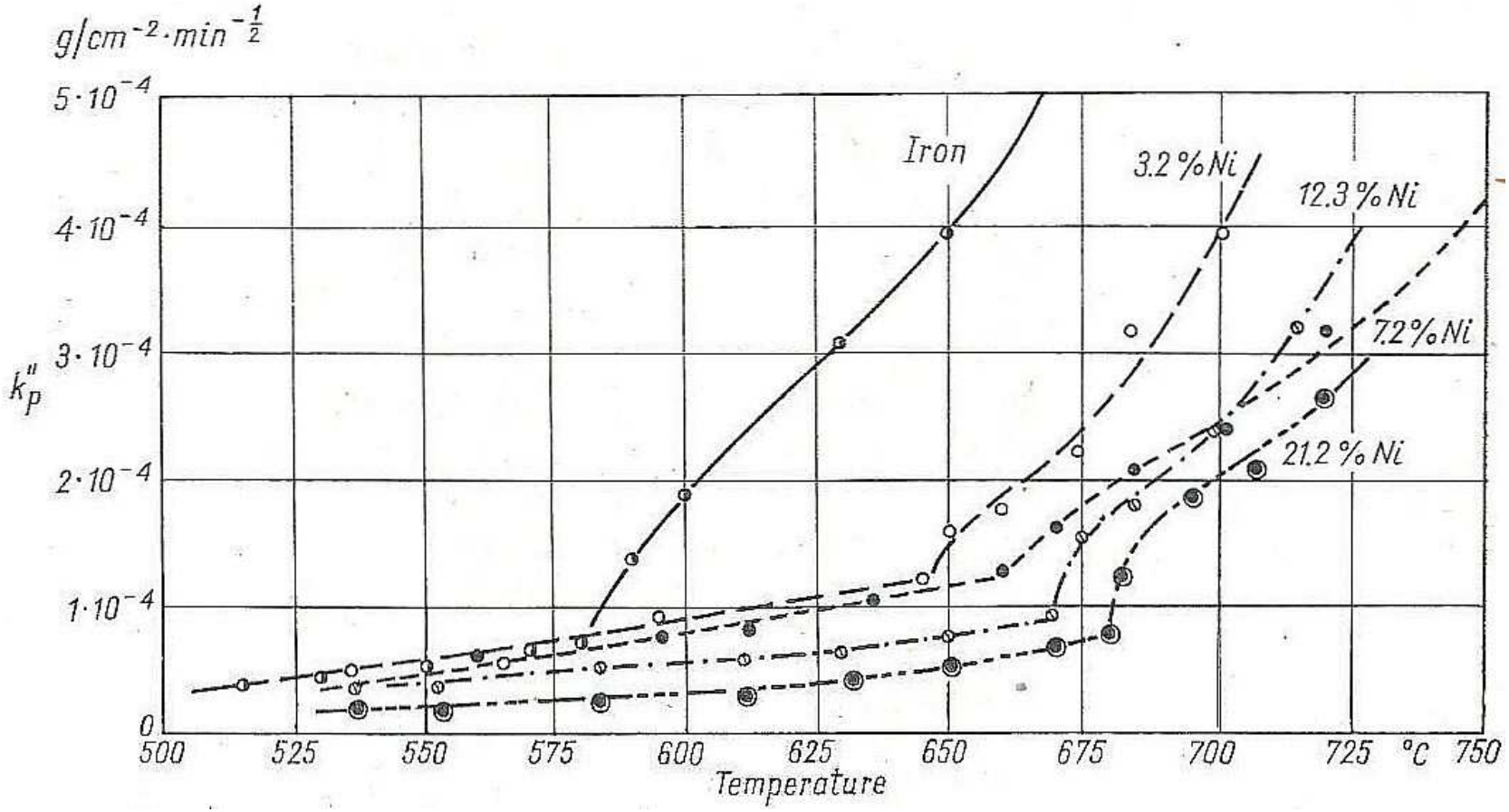

S. Mrowec, „An Introduction to the Theory of Metal Oxidation”, National Bureau of Standards and the National Science Foundation, Washington, D.C., 1982

Influence of the silicon dopant on the oxidation kinetics of an industrial kanthal Fe-Cr-Al alloy

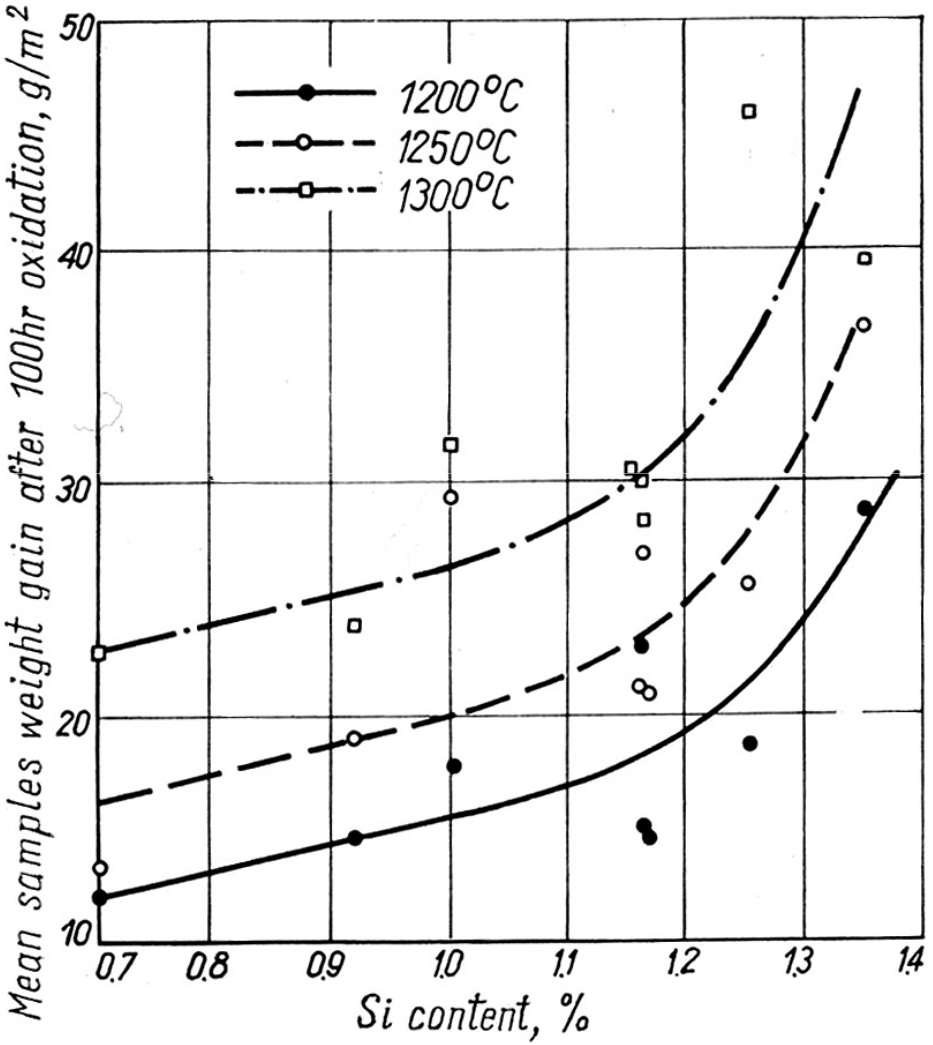

S. Mrowec, „An Introduction to the Theory of Metal Oxidation”, National Bureau of Standards and the National Science Foundation, Washington, D.C., 1982

THE END